Available online at www.sciencedirect.com
SCIENCE DIRECT
Carbohydrate Polymers 65 (2006) 42–48
Carbohydrate Polymers
www.elsevier.com/locate/carbpol

Electron microscopic studies on planar texture and disclination of cholesteric mesophases in acyloyl chitosan/acrylic acid composite films

Yan-ming Dong *, Wei Mao, Hui-wu Wang, Ya-qing Zhao, Dan-xia Bi, Liu-lin Yang, Qiang Ge, Zi-qi Ou

Department of Materials Science and Engineering, Xiamen University, Xiamen 361005, China

Received 3 August 2005; received in revised form 6 September 2005; accepted 2 December 2005
Available online 12 May 2006

Abstract

A novel amphiphilic chitosan derivative, acryloyl chitosan (AcCs), was synthesized by a homogeneous reaction of chitosan and acryloyl chloride using methanesulfonic acid as solvent and catalyst. The concentrated solutions of AcCs/acrylic acid were investigated by polarized optical microscopy (POM) and found demonstrate cholesteric mesophase above the critical concentration of 45 wt%. AcCs/polyacrylic acid (PAA) composite films were prepared via the photopolymerization of 52 wt% AcCs/acrylic acid solution, and subsequently the permanganic etching technique was employed to expose the textures and defects inside the composite films. The Grandjean planar textures were observed by POM, but a series of dark and bright striation lines, which were attributed to the periodic structure of the cholesteric helix, were detected by scanning electron microscopy (SEM). The disclination pairs, $\tau^{-}\lambda^{+}$ and $\tau^{+}\lambda^{-}$, were found, however $\lambda^{+}\lambda^{-}$ and $\tau^{+}\tau^{-}$ were absent. Effect of etching time on morphology of AcCs/PAA composite films was also investigated, comparing with 30 wt% free-acetyl chitosan (CS)/PAA composite films. The results showed that AcCs/PAA composite films had better anticorrosion ability than (CS)/PAA composite films, due to the crosslinking network between AcCs and PAA. FTIR confirmed that double bonds of AcCs involved in photo-solidification. Therefore the system studied takes the advantage of easy controlling for permanganic etching.

Keywords: Acryloyl chitosan; Cholesteric liquid crystals; Texture; Disclination; SEM; Permanganic etching

1. Introduction

Chitosan, poly [β-(1→4)-2-amino-2-deoxy-D-glucose], is an aminopolysaccharide normally obtained by alkaline deacetylation of chitin which is the second most abundant natural macromolecules except cellulose. Like other biopolymers, such as polypeptides, DNA, RNA, cellulose and so on, chitosan and most of its derivatives can form lyotropic cholesteric liquid crystalline phases in appropriate solvents. The structure of a cholesteric liquid crystalline phase is showed in Scheme 1a. The rod-like molecules predominantly orient along one director in each layer and the layers of rod-like molecules are parallel to each other but successively turn a small angle from one layer to the next (Werbowyj & Gray, 1984).

Since 1982, the lyotropic mesophases of chitosan and its derivatives have been studied by some groups. Ogura et al. (1982) reported that chitosan (hydroxyrpopyl) chitosan and (acetoxypropy1) chitosan form cholesteric phase at concentrated solutions. Sakurai, Shibano, Kimura, and Takahashi (1985) studied liquid crystalline structure in the films and fibers of chitosan prepared from liquid crystalline solutions (Sakurai et al., 1985, 1988; Sakurai, Miyata, & Takahashi, 1990). Rout et al. (Rout, Barman, Pulapura, & Gross, 1994; Rout, Pulapura, & Gross, 1993a,b) found cholesteric solution in *N*-phthaloyl chitosan and *N*-phthaloyl-3,6-di-*O*-acetyl chitosan dissolved in organic solvents. Ratto et al. (1995) investigated the mesophase of water/chitosan systems with differential scanning calorimetry. Dong et al. (Dong and Wang, 2000; Dong and Yuan, 2000) demonstrated lyotropic liquid crystallinity of some chitosan derivatives and investigated the influences of the structure factors such as molar mass and degree of substitution of these derivatives on critical concentration forming liquid crystal phases (Dong & Li, 1999; Dong and Wang, 2000). Studies on the structure and morphology of chitosan lyotropic cholesteric liquid crystalline phases are important to the

* Corresponding author. Tel.: +86 059 2218 6095; fax: +86 059 2218 3937.
E-mail address: ymdong@xmu.edu.cn (Y.- Dong).

0144-8617/$ - see front matter © 2006 Published by Elsevier Ltd.
doi:10.1016/j.carbpol.2005.12.007

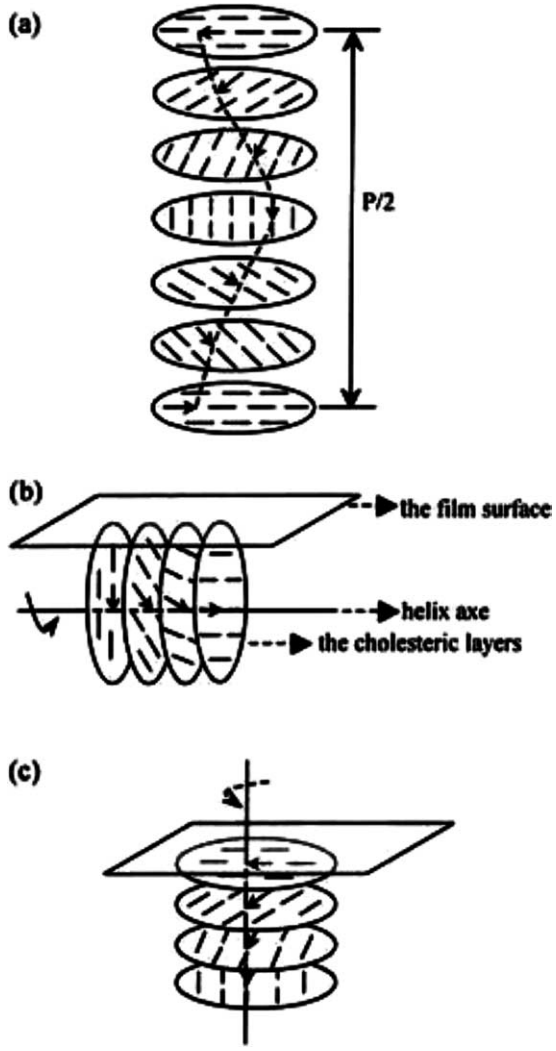

Scheme 1. (a) Schematic arrangement of the molecules in the cholesteric liquid crystalline phase (P pitch of the helix); (b) Schematic arrangement of the molecules in fingerprint-like texture under POM; (c) Schematic arrangement of the molecules in Grandjean planar texture under POM.

application of chitosan for their influences on the rheological and optical properties of this material. Cholesteric liquid crystalline phases usually demonstrate fingerprint-like texture or Grandjean planar texture under polarized optical microscopy (POM). The former is a typical texture of cholesteric mesophases in which the helix axes are parallel to the sample surface (Scheme 1b). However, the latter is the most frequent texture, in which the helix axes are parallel to the sample surface but the pitch is much smaller than wave length, or the helix axes perpendicular (or slightly tilt) to the film surface (Scheme 1c), since the long rigid or semi-rigid molecules lie preferentially parallel to the film surface. The structure of fingerprint-like texture of chitosan derivatives has been delicately studied by POM and scanning electron microscope (SEM) (Dong, Wang, & Yuan, 2000; Dong, Wu, Yuan, Yuan, & Wang, 2000; Dong, Yuan, Wu, & Wang, 2000; Dong, Yuan, & Huang, 2000). Nevertheless the structure of the Grandjean planar texture of chitosan or its derivatives has not been particularly paid attention. In this paper, a novel chitosan derivative, acryloyl chitosan (AcCs) with active side vinyl groups was synthesized. The Grandjean planar texture of AcCs/polyacrylic acid composite film was investigated by means of POM and SEM. The latter allowed direct observations of Grandjean planar texture after chemical etching.

2. Experimantal section

2.1. Materials

Commercial reagent-grade chitosan (from crab shell) with degree of deacetylation 91% (determined by acid-base titration method) and viscosity average molecular weight 4.5×10^5, supplied by Shandong Chitin Powder Factory (China), was used after a full deacetylation treatment with the method proposed by Shigehiro et al. (1994). The degree of deacetylation was almost 100% (determined with FTIR method) after this process. The complete deacetylation chitosan was then used for the synthesis of acryloyl chitosan (AcCs).

2.2. Synthesis of AcCs

A 2.1 g (about 13 mmol) amount of chitosan powder was added to 11 mL methanesufonic acid with stirring at −2–0 °C for 2 h. acryloyl chloride of 10 mL was added dropwise to the gel of chitosan in methanesufonic acid. The mixture was stirred at 0 °C for 4 h, and kept at −18 °C overnight. The product, precipitated by pouring into acetone, was filtered and extracted in a Soxhlet apparatus over acetone for 18 h to remove impurities. Then the precipitate was further purified by reprecipitation from a methanol solution into acetone. The product was dried in vacuo at room temperature with the presence of P_2O_5 for 24 h, and then stored in dark.

The infrared spectra were measured with a Nicolet Avator 360 FTIR by the KBr pellet method. ^{1}H NMR results were obtained with a Varian Unity NMR Spectrometer at 500 MHz, D_2O was used as solvent.

2.3. Solution and composite preparation

Solutions were prepared from 40 to 50 wt% (1 wt% interval) of AcCs/acrylic acid (AA) for liquid crystal critical concentration determination using an Olympus BH-2 POM.

The glass vials were sealed with 52wt% AcCs and 30 wt% CS solution in AA (including 5 wt% benzoin ethyl ether as initiator and a small amount of water that was necessary for solvation) respectively. Both solutions were left to homogenize for 2 days at room temperature in darkness. The solutions were then sandwiched between two small slides with a thickness of about 30 μm and photopolymerized using an ultraviolet chamber equipped with a 250 W high-intensity mercury arc lamp for 5 min to form solidified AcCs/PAA and CS/PAA composite films. One of the glass slides was removed to expose the surface of the films. After that, the films were etched by a solution of 0.7 wt% $KMnO_4$ in a 2:1 mixture of H_2SO_4 and H_3PO_4 (85%) for certain time, then washed by 30% H_2O_2 aqueous solution and distilled water and dried in the air.

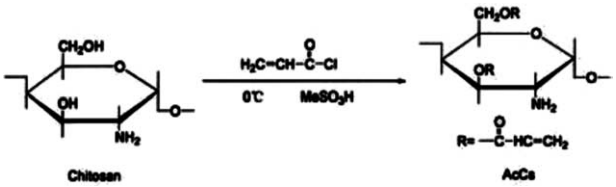

Scheme 2. Schematic illustration ofAcCs preparation.

An Olympus BH-2 POM and a DXS-10A SEM were used for investigation.

3. Results and discussion

3.1. Characterization of AcCs

AcCs was prepared by a homogenous reaction of chitosan and acryloyl chloride using methanesulfonic acid as solvent and catalyst in low temperature. Acidic condition (methanesulfonic acid as solvent) is disadvantageous for the nucleophilic displacement reaction of amino group which has been protonated. Therefore, the acryloylation is supposed to happen preferentially onto the hydroxyl groups (see Scheme 2). This has been confirmed by FTIR results (showed in Fig. 1).

Compared with completely deacetylated chitosan, the structure of AcCs was verified by ν(C=O) 1.731 cm^{-1} of ester group, ν(C=C) 1634 cm^{-1}, β(C=C) 1410 cm^{-1} and γ(=CH) 806, 782 cm^{-1}. Almost absence of $\nu(C_6–OH)$ 1026 cm^{-1} and $\nu(C_3–OH)$ 1088 cm^{-1} and unchanged $\nu(C_2–NH_2)$ 1600 cm^{-1} illustrated that the substitution mainly happened at hydroxyl groups.

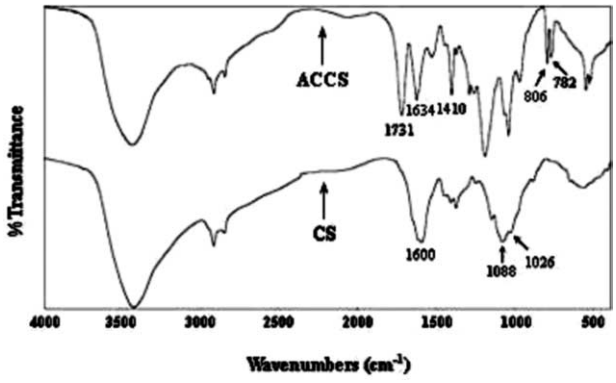

Fig. 1. FTIR spectra of acetyl-free chitosan and AcCs.

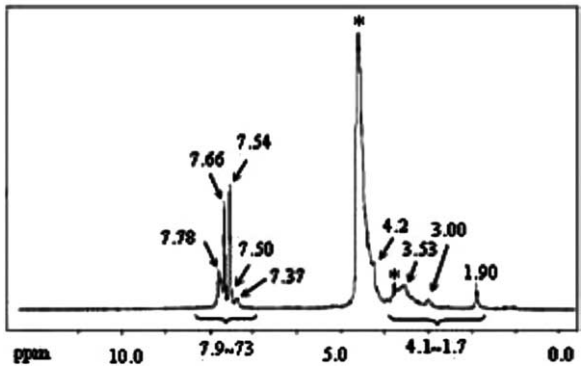

Fig. 2. ^{1}H NMR spectrum of AcCs.

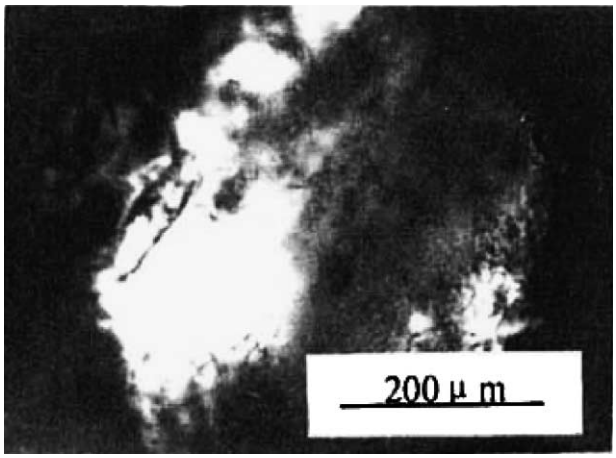

Fig. 3. POM photograph of Grandjean planar texture in 52 wt% AcCs/AA concentrated solution.

The ^{1}H NMR (D_2O, ppm) spectrum of AcCs (Fig. 2) shows resonance signals at δ7.3–7.9 ppm (m, 3H) corresponding to the protons of –CO–CH=CH_2, δ1.7–4.1 ppm (m, 6H) corresponding to the protons of C6, C6′, C5, C4, C3, C2 and δ4.2 (m, 1H) corresponding to the protons of C1 in pyranose ring. The last is a shoulder peak on the huge resonance signals of D_2O (δ4.6). The degree of substitution was about 1.96 per glucose unit via the calculation of the integral ratio of δ7.3–7.9 and δ1.7–4.1 ppm.

3.2. Liquid crystal critical concentration determination of AcCs/AA

A unique property of AcCs is its solubility in both water and common organic solvents such as formic acid, formamide, MeOH and AA. AcCs exhibited lyotropic liquid crystalline phases in concentrated AA solutions. Fig. 3 showed Grandjean

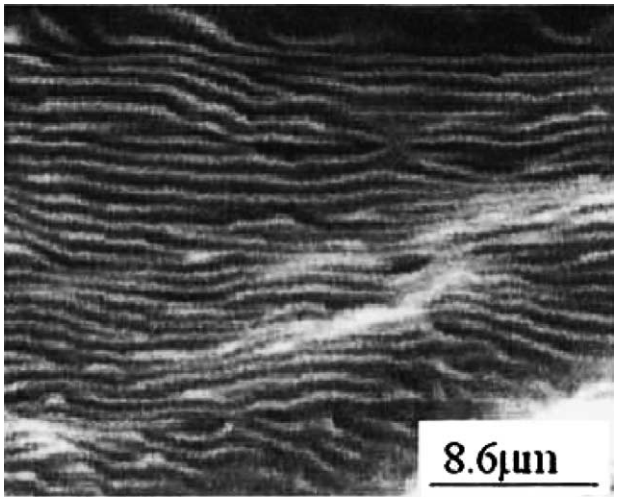

Fig. 4. SEM Photograph of fingerprint-like texture of 52 wt% AcCs/PAA composite film via permanganic etching.

planar texture in 52 wt% AcCs/AA concentrated solution, which is typical for cholesteric; phases. The liquid crystal critical concentration determined by POM was 45 wt%.

3.3. Texture and disclination of AcCs/PAA composite films

AA is a polymerizable solvent. After photo polymerization, the sample films remained opalescent and the cholesteric order in the solution was retained in the solid AcCs/PAA composite films. The side double bonds of AcCs was responsible for ease of solidification. The AcCs/PAA composite film demonstrated dark and bright striation lines, which were attributed to periodic structure of the cholesteric helix, observed by SEM after permanganic etching (showed in Fig. 4). The space between two striation lines was about 1 (m, which well corresponded to a half of the pitch lengths. No fingerprint-like textures but only Grandjean planar textures could be seen in the AcCs/PAA composite films under POM. Because in this case the pitch lengths of cholesteric mesophases was too small to be distinguished by POM, it was regarded as so-called Grandjean planar texture. But by use of SEM the fine striation lines, so-called fingerprint pattern were clearly observed.

The defects such as disclinations of cholesteric layer texture can be elucidated from the micrographs×perpendicular disclinations were observed in AcCs/PAA composite films× perpendicular disclinations have been split into disclination pairs which is necessary for remaining lower energy (Xie, 1998) (showed in Figs. 5 and 6). The types of disclination in AcCs/PAA composite films observed were very simple. Only two kinds of disclination pairs $\lambda^{-}\tau^{+}$ and $\lambda^{-}\tau^{+}$ were found. No single disclination, λ or τ, and other χ disclinations, $\lambda^{-}\lambda^{+}$ or $\tau^{-}\tau^{+}$ were observed which have presented in composite films of other chitosan derivatives, such as *O*-cyanoethyl chitosan (Dong, Wang et al., 2000; Dong, Wu et al., 2000; Dong, Yuan et al., 2000; Dong, Yuan, & Huang, 2000). Although SEM measurements have provided the results that disclination pairs $\lambda^{-}\tau^{+}$ and $\tau^{-}\lambda^{+}$ were the more frequent configurations, it is still unclear why they were dominant in AcCs systems.

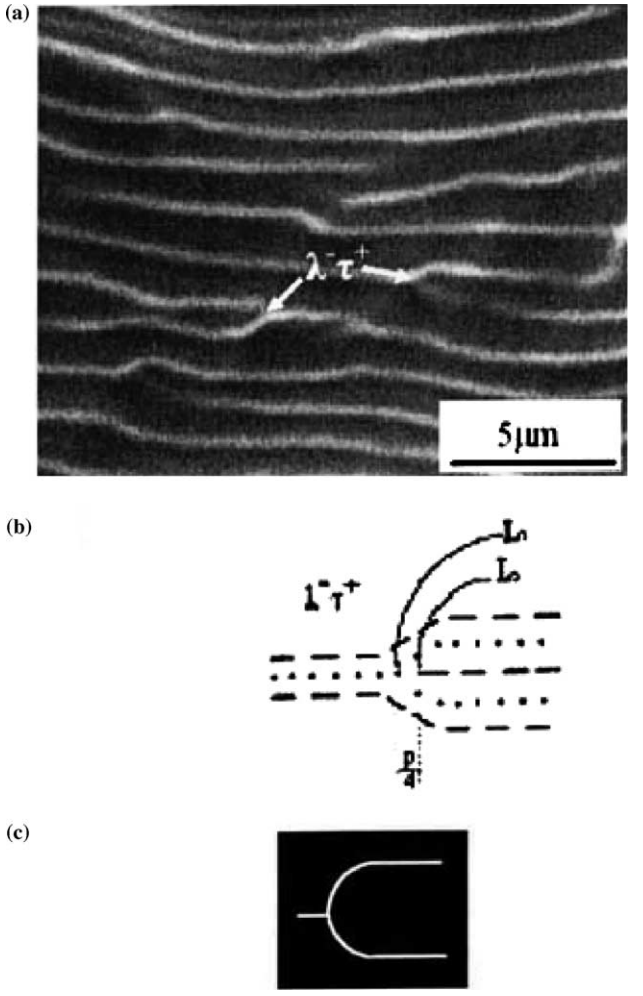

Fig. 5. The perpendicular disclinations of χ®$\lambda^{-}+\tau^{+}$ (i.e. $\lambda^{-}\tau^{+}$). (a) SEM photograph of this disclination pairs; (b) schematic structure of this disclination pairs (the dashes represent the directors parallel to the paper plane, while the dots represent the directors perpendicular to the paper plane); (c) schematic picture shown in SEM photograph.

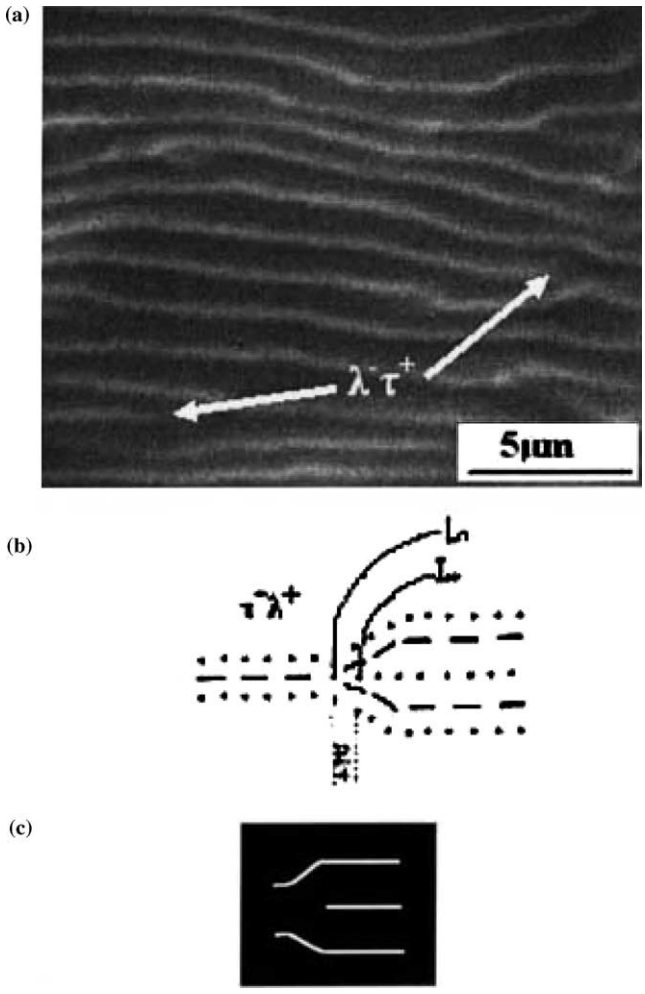

Fig. 6. The perpendicular disclinations of χ®$\tau^{-}+\lambda^{+}$ (i.e. $\tau^{-}\lambda^{+}$). (a) SEM photograph of this disclination pairs; (b) schematic structure of this disclination pairs (the dashes represent the directors parallel to the paper plane, while the dots represent the directors perpendicular to the paper plane); (c) schematic picture shown in SEM photograph

3.4. Effect of etching time on morphology of AcCs/PAA

The morphology studies of the solid cholesterics have been widely examined by using the transmission electron microscopy method for cellulose derivatives (Hara et al., 1988; Huang et al., 1998; Wang & Huang, 2000; Arrighi, Cowie, & Vaqueiro, 2002; Wang & Huang, 2004). Compared with ultra-microtome technique which was still under debate for the inevitable sectioning artifacts arising from shrinkage and deformation stress present in ultrathin slices, permanganic etching technique has deemed to be an excellent preparation technique of specimen preparation for SEM in the study of both conventional crystalline polymers such as polyolefine (Olley et al., 1979; Olley and Bassett; 1988) and nematic liquid crystalline polymers such as polyesters (Ford et al., 1990) with less artifacts and easier explanation of surface topography. The origin of the contrast in SEM is as follows. When the composite films were rendered for permanganic etching, the molecules laying on the surface of the film were much easier to be attacked for the chain scission and salvation of the resulting fragments, but the molecules being normal to the surface of the film were rather more resistant to be degraded for the formation of oxidized end groups (usually –COOH). Therefore the molecules on the dark lines presumably lie parallel to the plane of micrographs.

However, most of chitosan derivatives are very easy to decay, and the etching process is hard to control. In order to illustrate the anticorrosion ability to permanganic etching, effect of etching time on morphologies of AcCs/PAA and free-acetyl CS/PAA composite films were compared. The

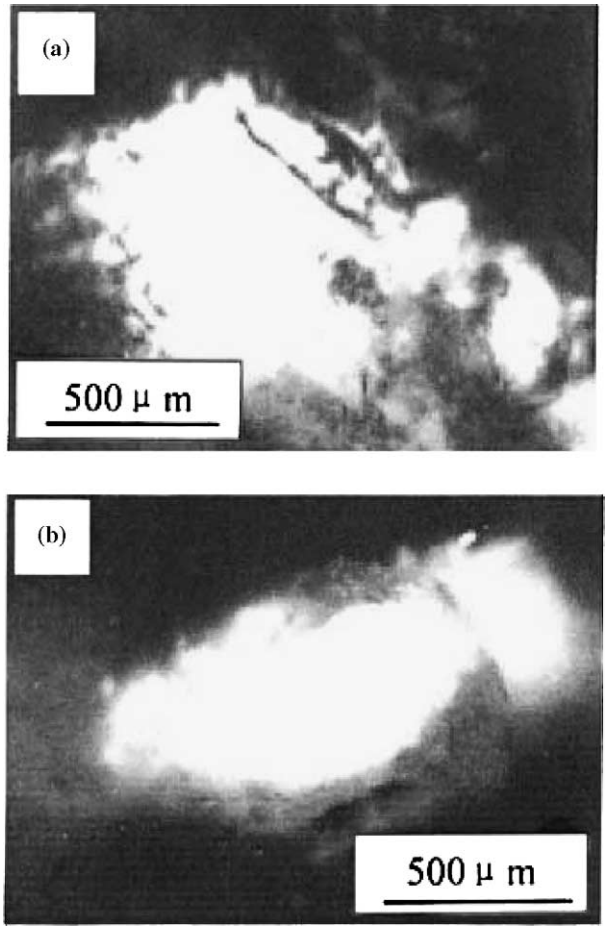

Fig. 7. POM photographs of the cholesteric liquid crystalline phases in the AcCs/PAA composite films. permanganic etching time (a) $t=70$ min; (b) $t=50$ mins.

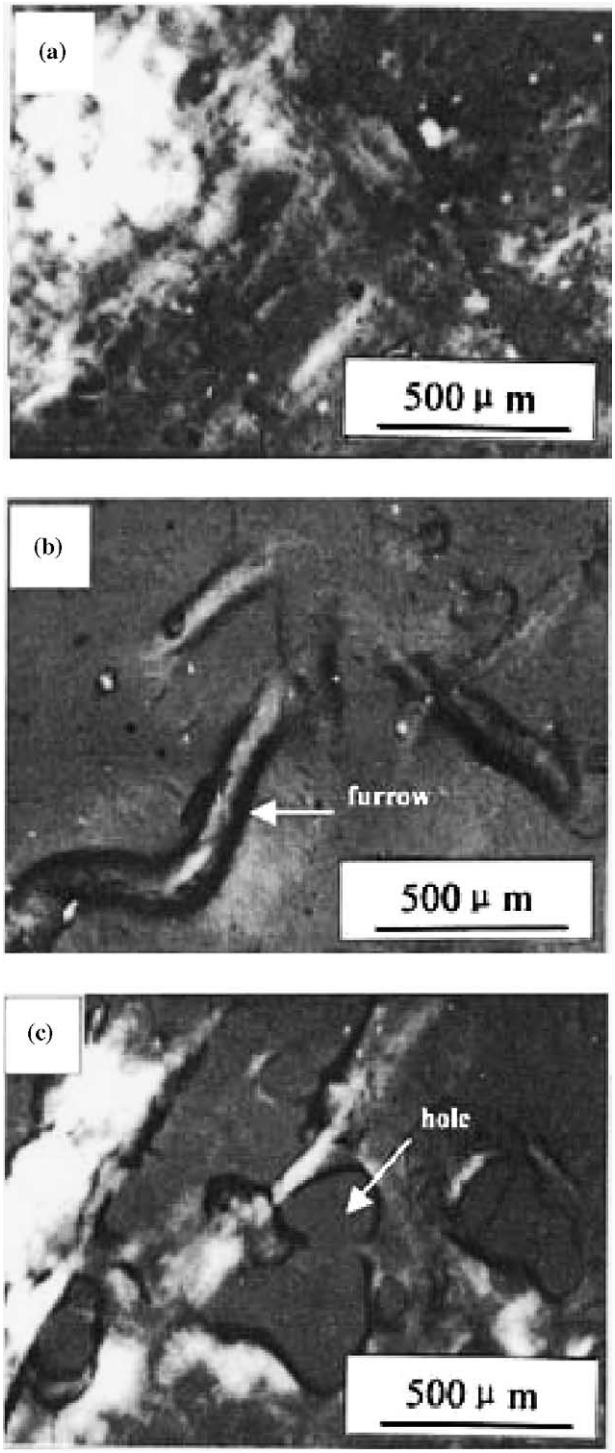

Fig. 8. POM photographs of the morphologies in CS/PAA composite films. permanganic etching time (a) $t=0$ min; (b) $t=20$ min; (c) $t=30$ min.

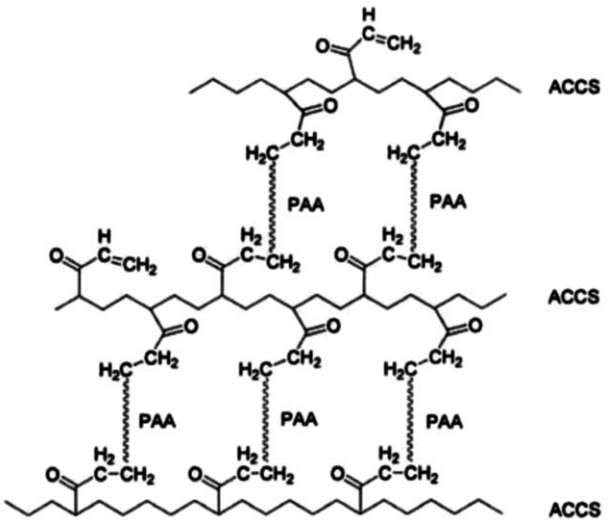

Scheme 3. Schematic structure of the network in AcCs/PAA composite films.

AcCs/PAA composite films demonstrated outstanding anticorrosion ability to permanganic etching. They kept unchanged and preserved the integrity of the film after permanganic etching for 50 min (Fig. 7). However the CS/PAA composite films swelled after permanganic etching for 5–15 min; part of the texture destroyed, the furrow and hole appeared in the films after permanganic etching for more than 20 min (Fig. 8). Therefore the system studied takes the advantage of easy controlling for permanganic etching.

The excellent anticorrosion ability to permanganic etching of AcCs/PAA lied on the special molecular structure of AcCs. The unsaturated double bond of AcCs took part in the photopolymerization of AcCs/AA composite films and a network of AcCs and PAA were obtained. The schematic structure of the network in the AcCs/PAA composite film was showed in Scheme 3. Double bond of AcCs took part in the forming of photopolymerization in AcCs/PAA composite film could be further confirmed by FTIR spectra. As showed in Fig. 9, 806 and 782 cm^{-1}, belonged to γ (=CH) of unsaturated double bond in AcCs were almost disappeared, and 1635 cm^{-1} of ν(C=C) and γ (N–H) in AcCs moved to 1627 cm^{-1} of γ (N–H) in AcCs/PAA composite film.

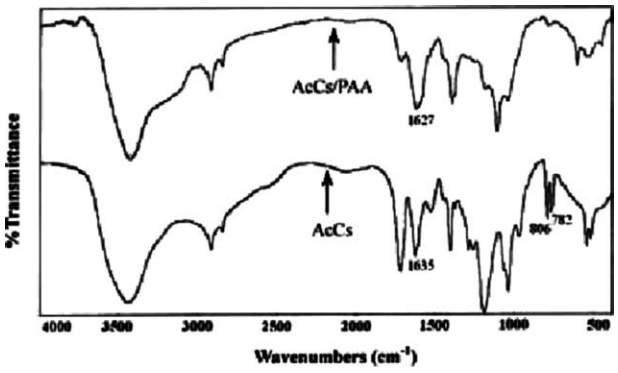

Fig. 9. FTIR spectra of AcCs and AcCs/PAA composite films.

4. Conclusions

We have synthesized a novel amphiphilic chitosan derivative, AcCs, by a homogeneous reaction of chitosan and acryloyl chloride using methanesulfonic acid as solvent and catalyst. The concentrated solutions of AcCs/acrylic acid demonstrated Grandjean planar texture, a typical cholesteric texture, above its critical concentration of 45 wt%. A finger print-like texture with a series of dark and bright striation lines in AcCs/polyacrylic acid (PAA) composite films, which were prepared via photopolymerization of 52 wt% AcCs/acrylic acid solution and permanganic etching technique, was found by means of SEM. The disclination pairs, $\tau^{-}\lambda^{+}$ and $\tau^{+}\lambda^{-}$, were also distiguished from the texture. AcCs/MA composite films had better anticorrosion ability compared with free-acetyl chitosan (CS)/PAA composite films due to the forming of crosslinking network between AcCs and PAA.

5. Uncited references

Olley et al. (1986). Sakurai and Takahashi (1988).

Acknowledgements

The authors gratefully acknowledge the National Natural Science Foundation, China (20374041), the Natural Science Foundation of Fujian, China (E0310002, E0510003) and the key Project of Science and Technology of Fujian, China (20041006), for financial support.

References

Arrighi, V., Cowie, J. M. G., & Vaqueiro, P. (2002). Fine structure and optical properties of cholesteric films prepared from cellulose 4-methylphenyl urethane/N-vinyl pyrrolidinone. *Macromolecules*, *35*, 7354–7360.

Dong, Y., & Li, Z. (1999). Lyotropic liquid crystalline behavior of five chitosan derivatives. *Chinese Journal of Polymer Science*, *17*, 65–70.

Dong, Y., Wang, J., & Yuan, Q. (2000). Influence of molecular weight of chitin and its three derivatives on critical concentration of lyotropic liquid crystalline phase transition. *Chinese Journal of Polymer Science*, *18*, 15–17.

Dong, Y., Wu, Y., Yuan, Q., Yuan, Y., & Wang, M. (2000). Studies on cholesteric liquid crystalline texture of chitosan and its derivatives with surface techniques. *Journal of Xiamen University*, *39*, 85–86.

Dong, Y., Yuan, Q., & Huang, Y. (2000). Texture and disclinations in the cholesteric liquid-crystalline phase of a cyanoethyl chitosan solution. *Journal of Polymer Science Physics Edition*, *38*, 980–986.

Dong, Y., Yuan, Q., Wu, Y., & Wang, M. (2000). Fine structure in cholesteric fingerprint texture observed by scanning electron microscopy. *Polymer Bulletin*, *44*, 85–91.

Ford, J. R., Bassett, D. C., Mitchell, G. R., & Ryan, T. G. (1990). Morphology of a main chain liquid crystal polymer containing semi-flexible coupling chain. *Molecular Crystal Liquid Crystal*, *180*, 233–243.

Hara, H., Satoh, T., Toya, T., Iida, S., Orii, S., & Watanabe, J. (1988). Cholesteric liquid-crystalline polyesters. 1. cholesteric: liquid-crystalline copolyesters based on poly(chloro-1, 4-phenylene trans-1,4-cyclo hexane dicarboxylate). *Macromolecules*, *21*, 14–19.

Huang, Y., Yang, Y., & Petermann, J. (1998). Atomic force microscopy on ethyl-cyanoethyl cellulose/polyacrylic acid composites with cholesteric order. *Polymer*, *39*, 5301–5306.

Ogura K., Kanamoto T., Sannan T., Tanaka K. & Iwakura Y. (1982). Liquid crystalline phases based on chitosan and its derivatives. *Chitin Chitosan Proceeding International Conference 2nd*, Japan: Tottoi, pp. 39–41.

Olley, R. H., Bassett, D. C., & Blundell, D. J. (1986). Permanganic etching of peek. *Polymer*, *27*, 344–348.

Olley, R. H., Hodge, A. M., & Bassett, D. C. (1979). A permanganic etchant for polyolefins. *Journal of Polymer Science: Polymer Physics Edition*, *17*, 627–643.

Ratto, J., Hatakeyama, T., & Blumstein, R. B. (1995). Differential scanning calorimetry investigaion of. phase transitions in water/chitosan systems. *Polymer*, *36*, 2915–2919.

Rout, D. K., Barman, S. P., Pulapura, S. K., & Gross, R. A. (1994). Cholesteric mesophases formed by the modified biological macromolecule 3,6-(butyl carbamate)-N-phthaloyl chitosan. *Macromolecules*, *27*, 2945–2950.

Rout, D. K., Pulapura, S. K., & Gross, R. A. (1993a). Liquid-crystalline characteristics of site -selectively- modified chitosan. *Macromolecules*, *26*, 5999–6006.

Rout, D. K., Pulapura, S. K., & Gross, R. A. (1993b). Gel-sol transition and thermotropic behavior of a chitosan derivative in lyotropic solution. *Macromolecules*, *26*, 6007–6010.

Sakurai, K., Miyata, M., & Takahashi, T. (1990). Fiber structure and tensile property of chitosan fiber spun from lyotropic liquid crystalline solution. *Sen-i Gakka ishi*, *46*, 79–81.

Sakurai, K., Shibano, T., Kimura, K., & Takahashi, T. (1985). Crystal structure of chitosan II. Molecular packing in unit cell of crystal. *Sen-i Gakka ishi*, *41*, T361–T368 (England).

Sakurai, K., & Takahashi, T. (1988). Banded structure and crystal structure in chitosan prepared from oriented lyotropic liquid crystalline solution. *Sen-i Gakka ishi*, *44*, 149–151 (Japan).

Shigehiro, H., Akinhirro, U., & Min, Z. (1994). Chitin xanthate and so me xanthate ester derivatives. *Carbohydrate Research*, *256*, 331–336.

Xie, Y. (1998). *The physics of liquid crystals (in Chinese)*. Beijing: Science Press.

Wang, L., & Huang, Y. (2000). Effects of magnetic field on ethyl-cyanoethyl cellulose cholesteric order. *Macromolecules*, *33*, 7062–7065.

Wang, L., & Huang, Y. (2004). Structural characteristics and defects in ethyl-cyanoethyl cellulose/acrylic acid cholesteric liquid crystalline system. *Macromolecules*, *37*, 303–309.

Werbowyj, R. S., & Gray, D. G. (1984). Optical properties of (hydroxypropyl) cellulose liquid crystals. Cholesteric pitch and polymer concentration. *Macromolecules*, *17*, 1512–1520.